Journal of Zhejiang University-SCIENCE A (Applied Physics & Engineering)
ISSN 1673-565X (Print); ISSN 1862-1775 (Online)
www.jzus.zju.edu.cn; www.springerlink.com
E-mail: jzus@zju.edu.cn

$NiCo_2O_4$ nanoparticles: an efficient and magnetic catalyst for Knoevenagel condensation*

Yang-yang FANG, Xiao-zhong WANG†‡, Ying-qi CHEN, Li-yan DAI†‡

Zhejiang Provincial Key Laboratory of Advanced Chemical Engineering Manufacture Technology, College of Chemical and Biological Engineering, Zhejiang University, Hangzhou 310027, China

†E-mail: wangxiaozhong@zju.edu.cn; dailiyan@zju.edu.cn

Received Oct. 22, 2019; Revision accepted Dec. 12, 2019; Crosschecked Dec. 28, 2019

Abstract: The Knoevenagel condensation reaction has wide applications ranging from the manufacture of basic chemicals to pharmaceutical intermediates. In this study, we developed an efficient and magnetic bimetallic $NiCo_2O_4$ nanocatalyst by co-precipitation. When used in the Knoevenagel condensation between various benzaldehydes and malononitrile, the catalyst exhibited excellent catalytic performance with 99% conversion and 99% selectivity under mild conditions. It can be easily recovered with a magnet and recycled for 20 runs without significant loss of activity. We expect that the catalyst will find large-scale industrial applications.

Key words: $NiCo_2O_4$ catalyst; Spinel; Knoevenagel condensation; Heterogeneous catalysis
https://doi.org/10.1631/jzus.A1900535 **CLC number:** TQ138.1

1 Introduction

Knoevenagel condensation has been extensively adopted in the fields of fine chemicals, drugs, perfumes, and cosmetics (Sun et al., 2005; Chen et al., 2008; Xu et al., 2013). A variety of pharmaceutical intermediates have been developed such as opioid analgesics (Viveka et al., 2016) and anticancer (Ali et al., 2013), antiHIV (Kasralikar et al., 2015), and antidiabetic (Sharma et al., 2011) medicines, broadly extending the applications in the drug industry. For instance, cinnamic acid (Adisakwattana et al., 2008), via condensation of benzaldehyde and methane dicarboxylic acid, is attracting increasing attention in cancer research because of its potent pharmacological and medicinal properties.

For decades, chemists and researchers have been working to activate condensation reactions. Recent studies have focused on catalysts within high efficiency, emphasizing the optimization of catalytic performance and the process for conversion (Hua and Hu, 2004). Remarkable progress has been achieved by employing various homogeneous bases and inorganic salts, such as pyridine (Ying et al., 2015), ammonia (Xue et al., 2018), alkali hydroxides (Xie et al., 2015), and zinc salts (Jiang et al., 2009). However, homogeneous catalysis suffers from difficulties in separation and recovery, especially when expensive and toxic heavy metal compounds are used (Ladipo and Anderson, 1994), and its use in wastewater treatment processes is costly (Rubio-Clemente et al., 2015). These problems have received considerable attention in scale-up applications with respect to environmental and economic issues. Optimization and improvement of the intrinsic performance of homogeneous catalysts are needed for practical applications (Jameel et al., 2016). Hence, many modification technologies have been used to extend the properties

‡ Corresponding author
* Project supported by the Fund of Zhejiang Provincial Key Laboratory of Advanced Chemical Engineering Manufacture Technology (No. 2017E10001), China
ORCID: Yang-yang FANG, https://orcid.org/0000-0001-9331-7231; Li-yan DAI, https://orcid.org/0000-0001-8084-0226

of catalysts to fulfill facile isolation. Various support materials such as C_3N_4 (Liu et al., 2017), γ-Al_2O_3 (Texier-Boullet and Foucaud, 1982), mesoporous crystalline material (MCM) (Sirotin et al., 2011), Santa Barbara, USA (SBA) (Burri et al., 2007), and organic polymers (Modak et al., 2013) have been employed, obtaining good to excellent results. The use of heterogeneous catalysts such as ZnO (Tamaddon and Azadi, 2017), Al_2O_3 (Wang et al., 2002), and MgO/ZrO_2 (Gawande and Jayaram, 2006) also shows great effects in transformation. However, when the diameter decreases to nanoscale, the same problems of separation and recovery may occur, as the nanoparticles can be evenly dispersed into solvent and form a relatively stable emulsion. Up to now, the developing magnetic catalysts, such as γ-Fe_2O_3 (Zhang and Xia, 2009), Fe_3O_4 (Karaoğlu et al., 2012), Mg-Fe (Gao et al., 2010), and $MgFe_2O_4$ (Ghomi and Akbarzadeh, 2018) have gained considerable attention owing to their easy and quick removal and high reactivity. Li et al. (2016) previously reported some magnetic MFe_2O_4 (M=Ni, Co, Cu, Mn, Zn) which exhibits strong ferromagnetism and achieves excellent conversion and selectivity simultaneously. Although there have been many high-performance catalysts, the development of effective and practically continuous methods for Knoevenagel condensation still remains a challenge.

Here, we tailored the structure and catalytic properties of magnetic $NiCo_2O_4$ nanoparticles to activate the condensation reaction between benzaldehyde and malononitrile with high efficiency at room temperature. Unlike previous catalysts, the nanocatalyst is active and stable in methanol and thus can be recycled for at least 20 runs without significant loss of activity. The $NiCo_2O_4$ catalyst has advantages of (1) outstanding catalytic activity with high selectivity and conversion, (2) notable stability for long-term usage, and (3) convenient processing under mild conditions and magnetic separation.

2 Experimental methods

2.1 General

All the chemicals used were purchased from Aladdin and Shanghai Hushi, China without further purification. Fourier transform infrared (FT-IR) spectroscopy was performed using a Nexus 670 spectrophotometer. X-ray diffraction (XRD) measurements were carried out on an X'Pert PRO X-ray diffractometer with Cu Kα radiation (from 10° to 80°). The crystalline structure of $NiCo_2O_4$ was further studied using an FEI Tecnai G2 F20 transmission electron microscope (TEM). The surface area and pore size of the catalyst were calculated with a Micromeritics Belsorp-mini II instrument (BET Japan, Inc), and temperature-programmed desorption (TPD) was performed using an AutoChem1 II 2920 at 100–550 °C. Gas chromatography (GC) was carried out using an Agilent 6820 gas chromatograph (FID detector, 30 m hp-5 capillary column). The target products were analyzed using an AVANCE III 500 ^{1}H nuclear magnetic resonance (^{1}H NMR), and melting points were recorded using a WRS-1B digital melting point apparatus.

2.2 Catalyst preparation

$NiCo_2O_4$ was synthesized via a coprecipitation method. Typically, 4 mmol $Ni(Ac)_2{\cdot}4H_2O$, 8 mmol $Co(Ac)_2{\cdot}4H_2O$, 20 mL ethylene glycol, and 48 mmol urea dissolved in 40 ml distilled water were mixed to form the solution A, followed by the addition of 1 mol/L NaOH under vigorous stirring at room temperature until the solution was neutral. The suspension was stirred at 90 °C for 4 h. Subsequently, the obtained precipitate was washed several times with distilled water and ethanol and then transferred into a muffle furnace and annealed at 350 °C in air for 4.5 h.

2.3 Knoevenagel condensation

A mixture of benzaldehyde (1 mmol), malononitrile (1.2 mmol), methanol (2 mL) as solvent, and $NiCo_2O_4$ nanopowder (8% in mol) as catalyst was magnetically stirred at room temperature. After 5 h of reaction, the $NiCo_2O_4$ was filtered using an external magnet and washed with methanol three times.

3 Results and discussion

3.1 Crystal structure of the $NiCo_2O_4$ catalyst

In spinel, AB_2O_4 is normally considered to have a face-centered cubic structure composed of O^{2-} ions in which A occupies one eighth and B occupies half of the octahedral sites. In contrast, $NiCo_2O_4$ is regarded as an inverse spinel (Sharona et al., 2017), exhibiting an opposite configuration in which Ni occupies the octahedral sites while Co is arranged in

both octahedral and tetrahedral sites. $NiCo_2O_4$ consists entirely of NiO_4 tetrahedra and Ni/CoO_6 octahedra (Fig. 1).

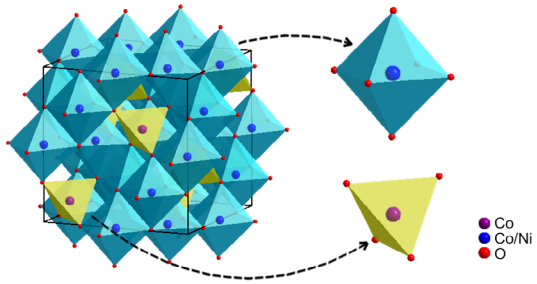

Fig. 1 Crystal structure of $NiCo_2O_4$. References to color refer to the online version of this article

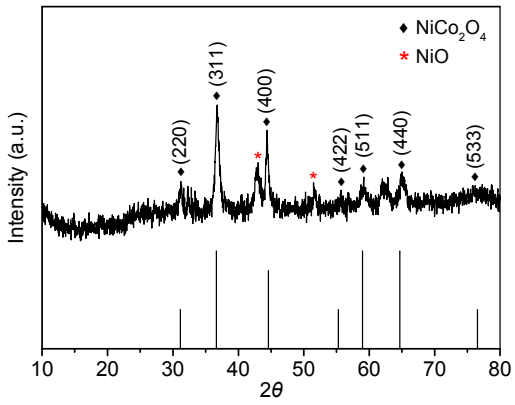

Fig. 2 XRD spectra of $NiCo_2O_4$ synthesized by the coprecipitation

3.2 Structure of $NiCo_2O_4$ catalyst

The properties of nickel cobaltite, $NiCo_2O_4$, standardly prepared by coprecipitation of nickel acetate and cobalt acetate, were examined by XRD, FT-IR spectroscopy (FT-IR), high-resolution transmission electron microscopy (HRTEM), brunauer emmett teller (BET), and TPD.

Fig. 2 shows the X-ray diffractogram of $NiCo_2O_4$ synthesized by coprecipitation. The sharp diffraction peaks at 31.1°, 36.6°, 44.6°, 55.3°, 59.0°, 64.7°, 76.6° are perfectly assigned to (220), (311), (400), (422), (511), (440), (533) reflections of the cubic spinel $NiCo_2O_4$ (JCPDS No. 02-1074), respectively. In addition, the mean size of the crystallites obtained from the Debye-Scherrer formula was found to be 16 nm. Significantly, the differences between $NiCo_2O_4$ and the standard sample were mainly in the impurity peaks of NiO, reasonably influenced by the calcination temperature. The control of calcination temperature is a critical factor affecting the degree of crystallization and the minimization of NiO generation. During the preparation, 350 °C was experimentally found to be optimal.

FT-IR spectra of $NiCo_2O_4$ composites are presented in Fig. 3. The two intense peaks around 657 and 563 cm^{-1} are derived from the M-O vibrations of tetrahedral and octahedral sites (Kaikhosravi et al., 2016). All the peaks observed can be assigned to the standard M-O bands (658–688 cm^{-1} and 553–603 cm^{-1}), showing a good agreement in the interval. Together with the XRD analysis, this demonstrates that cobaltites have been successfully prepared.

To obtain more detailed structural information, the morphological properties of the nano-$NiCo_2O_4$

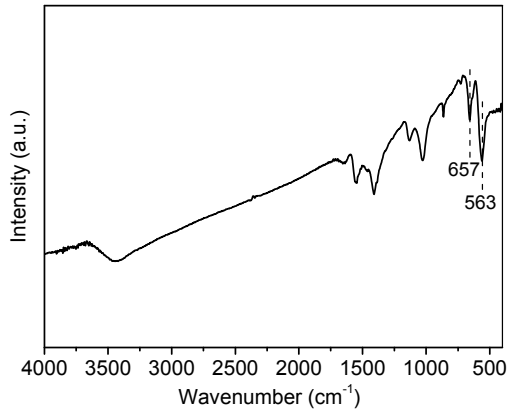

Fig. 3 FT-IR spectra of $NiCo_2O_4$ synthesized by the coprecipitation

catalyst were observed by TEM (Fig. 4). The TEM image shows that the particles are mostly spherical with average sizes ranging from 20 to 30 nm. Moreover, combined with the selected area electron diffraction (SAED) pattern, it can be clearly observed that $NiCo_2O_4$ shows a polycrystalline spinel structure, which is beneficial for the complete interaction of the active sites and the reactants. The sample shows lattice fringes with interplanar spacings (d) of 0.244 nm and 0.204 nm (Fig. 5), matching well with the expected spacings of 0.245 nm and 0.203 nm for the (311) and (400) lattice planes of $NiCo_2O_4$, respectively.

CO_2-TPD and NH_3-TPD were performed to evaluate the correlations between the quantity and strength of the base/acid sites and the chemical properties of the $NiCo_2O_4$ catalyst (Fig. 6). Two peaks appeared at 415.6 °C (Fig. 6a) and 413.5 °C (Fig. 6b), corresponding to strong base sites and strong acid

sites, respectively. In comparison, the peaks at lower temperatures were obviously very weak, suggesting few moderate and weak base/acid sites. Therefore, $NiCo_2O_4$ could be considered a kind of combined acid-base catalyst, which might provide a reasonable mechanism for the $NiCo_2O_4$ catalyzed Knoevenagel condensation.

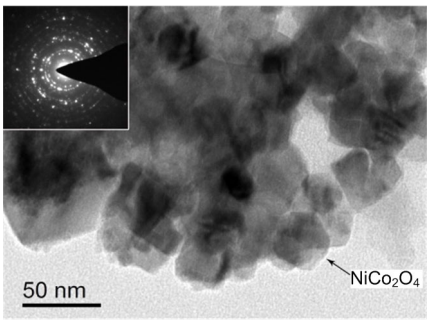

Fig. 4 TEM image and selected area electron diffraction (SAED) pattern of $NiCo_2O_4$ nanocatalyst

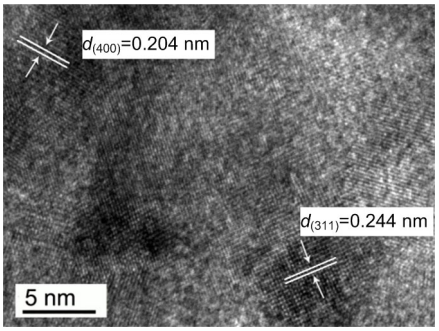

Fig. 5 HRTEM image of $NiCo_2O_4$ nanocatalyst

Fig. 7 shows the N_2 adsorption-desorption isotherm of the coprecipitated $NiCo_2O_4$. The sample shows a reversible IV isotherm with a type H3 hysteresis loop, which is one of the main characteristics of mesoporous materials. The surface area, pore volume, and pore size are listed in Table 1. The pore size distribution is mainly in the range of 2–5 nm using the adsorption branch by Barret-Joyner-Halenda (BJH) model, and can be seen more clearly in Fig. 8. A Multiwfn (Lu and Chen, 2012) was used to estimate and illustrate the dynamic diameters of benzaldehyde, malononitrile, and 2-[(E)-2-phenylethenyl]-propanedinitrile according to quantum theory (Fig. 9). The shape selectivity in $NiCo_2O_4$ spinel can improve a molecule's absorption and catalytic behavior. Taking Knoevenagel condensation for example, $NiCo_2O_4$ achieves the best catalytic performance when the kinetic minimum cross-sectional diameters of the molecules are close to, or smaller than, the $NiCo_2O_4$ composite's pore diameters.

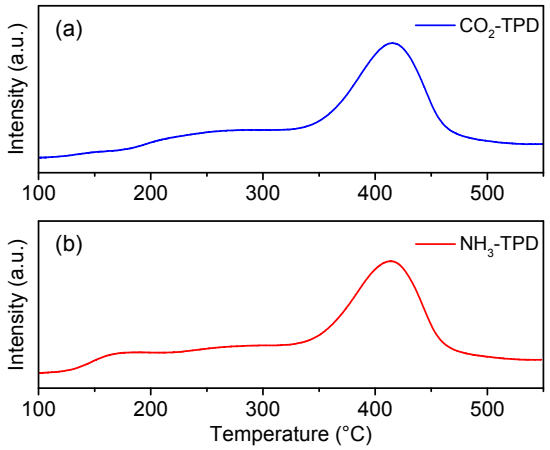

Fig. 6 CO_2-TPD (a) and NH_3-TPD (b) of the $NiCo_2O_4$ sample

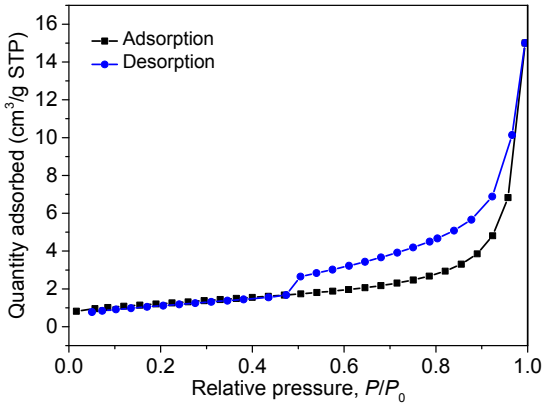

Fig. 7 N_2 adsorption-desorption isotherm of $NiCo_2O_4$

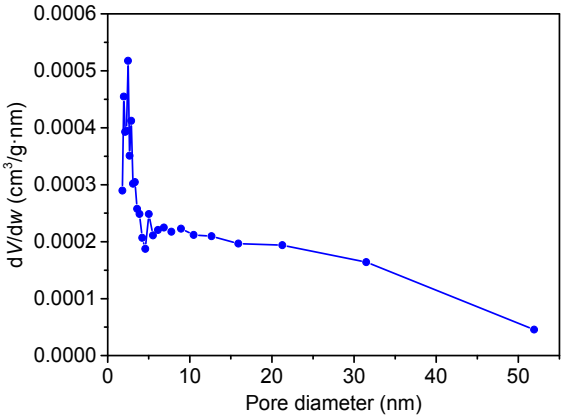

Fig. 8 Pore size distribution of $NiCo_2O_4$ (dV/dw indicates the incremental pore volume)

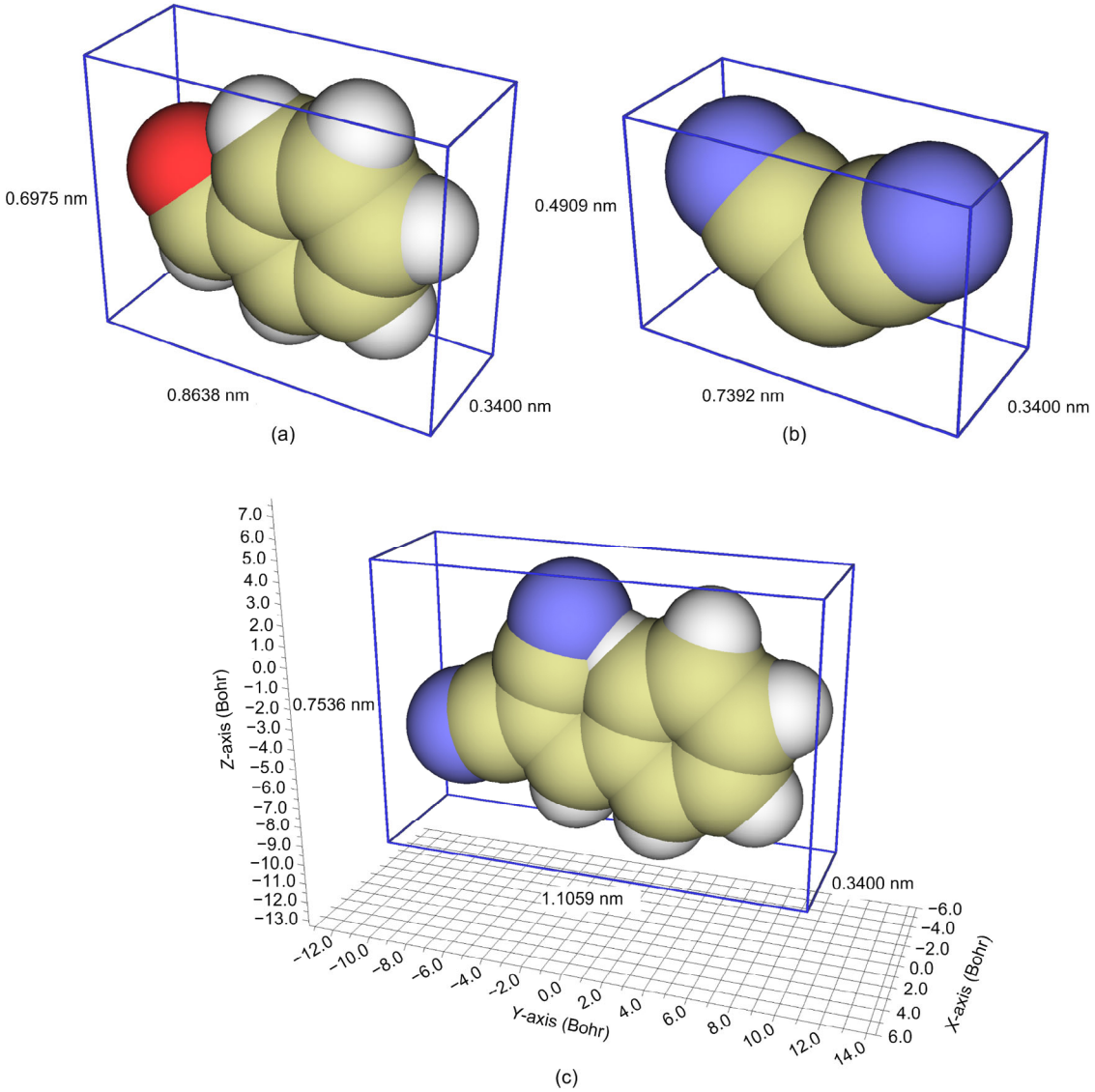

Fig. 9 Dynamic diameters of benzaldehyde (a), malononitrile (b), and 2-[(E)-2-phenylethenyl]propanedinitrile (c)

Table 1 Characteristics of the prepared $NiCo_2O_4$ catalyst

Sample	S_{BET} (m^2/g)	Pore size (nm)	Pore volume (cm^3/g)
$NiCo_2O_4$	4.302	21.263	0.023

S_{BET} refers to the specific surface area

3.3 Catalyst calcination

A series of $NiCo_2O_4$ samples were synthesized at different temperatures ranging from 250 to 450 °C, and were characterized by XRD and FT-IR. The XRD results of the freshly prepared catalysts are shown in Fig. 10. After the calcination process, the characteristic diffraction peaks of $NiCo_2O_4$ were clearly observed and the phase of NiO was present at 350 and 450 °C. The crystallinity of $NiCo_2O_4$ increased with temperature while an amount of NiO phase appeared and increased simultaneously, indicating $NiCo_2O_4$ could partially decompose at high temperatures. Thus, an appropriate calcination temperature was necessary to ensure a balance between crystallinity and purity.

To investigate the interactions of $NiCo_2O_4$ at different temperatures, FT-IR spectra were analyzed (Fig. 11). The characteristic adsorption bands at 657 and 563 cm^{-1} could be clearly found in $NiCo_2O_4$-350 and $NiCo_2O_4$-450, but were diminished in

$NiCo_2O_4$-250. Therefore, $NiCo_2O_4$ started to form an integrated spinel structure at about 250 °C and decomposed at 350 °C according to the XRD results. In addition, the differences between $NiCo_2O_4$-250, $NiCo_2O_4$-350, and $NiCo_2O_4$-450 were further characterized based on Knoevenagel condensation.

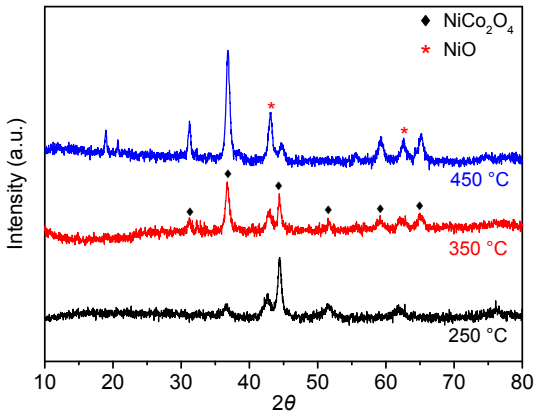

Fig. 10 XRD patterns of the prepared catalysts

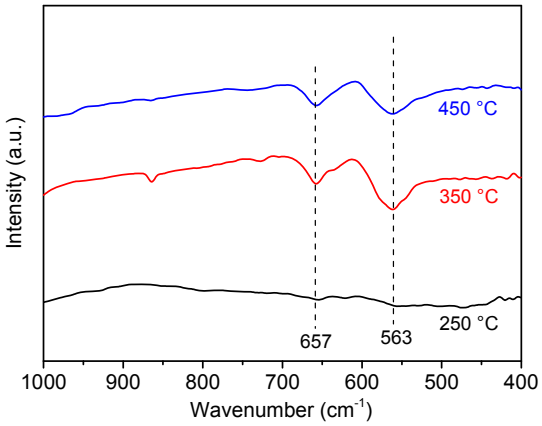

Fig. 11 FT-IR of the prepared catalysts

3.4 Catalytic performance for the Knoevenagel condensation

For the first time, the magnetic nano-$NiCo_2O_4$ was used as a heterogeneous catalyst for the Knoevenagel condensation of benzaldehyde and malononitrile at room temperature. A series of solvents including methanol, ethanol, N,N-dimethylformamide (DMF), tetrahydrofuran (THF), and toluene were used experimentally with good to excellent performance (Fig. 12). When toluene was used, the yield was only 58%, which might be attributable to the polarity of benzene because of its apparently symmetrical structure. In contrast, methanol was selected as the most promising solvent for the reaction because its yield of 99% was better than that of the other solvents.

To further investigate the practical reusability of the $NiCo_2O_4$ catalyst, recycling experiments were carried out with an optimal amount of 8% in mol for 5 h under the same reaction conditions. After each repeated cycle, the catalyst was separated by a magnet, washed with deionized water and methanol, and then dried at 60 °C for the next run. We observed that $NiCo_2O_4$ could activate the condensation, obtaining conversion and selectivity of up to 99% without a distinct decrease for 20 runs, far beyond some complex heterogeneous spinel catalysts listed in Table 2 (Gao et al., 2010; Li et al., 2016). Calcined $NiCo_2O_4$ exhibited high catalytic activity, but $NiCo_2O_4$-250 and $NiCo_2O_4$-450 decreased after four and five runs, respectively (Table 2, Entries 1, 2, and 3). Therefore, the fully retained performance of $NiCo_2O_4$-350, confirmed its great catalytic ability and practical stability. This phenomenon may well contribute to its good dispersion in methanol. Dai et al. (2011) reported that nanoparticles have a large surface area and high catalytic activity related to size effects and easily reunite after several reactions, which is the main obstacle in industrial applications of nano-materials. Taking into consideration the size effects (El Baydi et al., 1995; Pang et al., 2016), the spinel structure of $NiCo_2O_4$ shows superb chemical stability in the Knoevenagel condensation with the promise of good control of dispersion in methanol. An attractive benefit of the catalyst is its easy recovery using an external magnet (Fig. 13), which largely minimizes loss during recycling experiments.

The properties of the $NiCo_2O_4$ sample were evaluated by the recycling test and recovered for further FT-IR and XRD analysis. After recycling for 20 runs, the FT-IR spectrum of the $NiCo_2O_4$ catalyst was similar to that of freshly prepared nanoparticles, with characteristic peaks around 657 and 563 cm^{-1} (Fig. 14). XRD analysis was carried out to study the degree of crystallization and particle size, and confirmed that the intense peaks and the average crystallite size of $NiCo_2O_4$ showed no obvious differences after repeated use (Fig. 15). Hence, based on spinel structure, the catalyst appears to have superior stability and the potential to be used for longer reaction times while maintaining high quality.

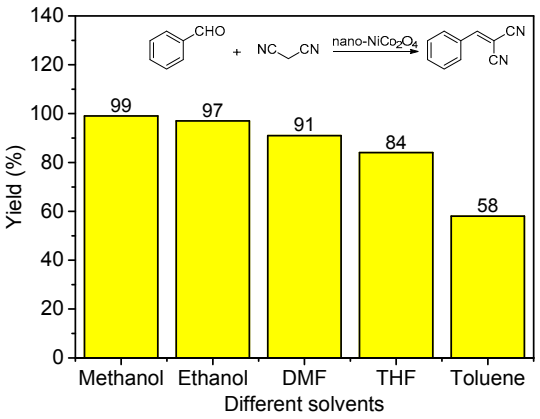

Fig. 12 Solvent effects on the Knoevenagel condensation reactions

Table 2 Catalyst effects on the Knoevenagel condensation of benzaldehyde and malononitrile[a]

Entry	Catalyst	Solvent	Reaction conditions	Yield[b] (%)	Cycle number
1	$NiCo_2O_4$-350	Methanol	r.t.,[c] 5 h	99	20
2	$NiCo_2O_4$-250	Methanol	r.t., 5 h	96	4
3	$NiCo_2O_4$-450	Methanol	r.t., 5 h	97	5
4	$NiFe_2O_4$	Ethanol	r.t., 5 h	98	8
5	$MgFe_2O_4$	Ethanol	r.t., 0.5 h	61	5
6	$CoFe_2O_4$	Ethanol	r.t., 5 h	96	–
7	$ZnFe_2O_4$	Ethanol	r.t., 5 h	95	–
8	$CuFe_2O_4$	Ethanol	r.t., 5 h	85	–
9	$MnFe_2O_4$	Ethanol	r.t., 5 h	85	–

[a] Reaction conditions: benzaldehyde (1.0 mmol) and malononitrile (1.2 mmol) catalyzed by different spinel catalysts; [b] The yield refers to that of the first cycle; [c] r.t. refers to room temperature

To explore expansion of the use of the catalyst, Knoevenagel condensations of various derivatives of benzaldehydes, followed by treatment with $NiCo_2O_4$ were prepared and resulted in satisfactory yields. In general, the reaction carried out using benzaldehyde and malononitrile (Table 3, Entry 1) gave a 99% yield in 5 h compared with only 77% in the blank without the catalyst, which gave much lower yields in the substituted experiments. While developing substituted chlorobenzaldehyde and methybenzaldehyde, the condensation reactions gave excellent yields with shorter times (Table 3, Entries 2, 3, 4, 5, and 6). In contrast, the reactions of ethyl cyanoacetate were slower because of the less active H, but yields remained high (Table 3, Entries 7, 8, and 9). Simultaneously, the melting points of all the products matched well with those previously reported (Voge and Good, 1949; Jiang et al., 2009; Zhang et al., 2013; Mahmoudi and Malakooti, 2014; Taher et al., 2016; Khan et al., 2017; Tryambake, 2017; Yang et al., 2018), suggesting that the catalyst has good potential for industrial applications.

Fig. 13 Magnetic separation of the $NiCo_2O_4$ nanocatalyst

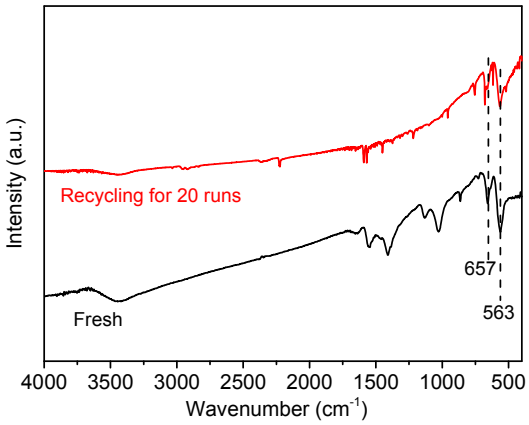

Fig. 14 FT-IR patterns of the fresh and used $NiCo_2O_4$ samples

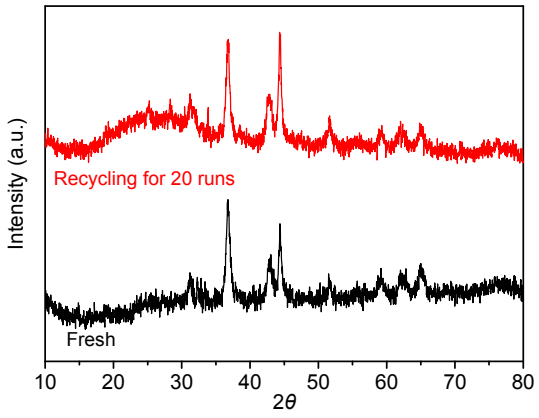

Fig. 15 XRD patterns of the fresh and used $NiCo_2O_4$ samples

Table 3 Knoevenagel condensation of benzaldehydes and malononitrile or ethyl cyanoacetate[a]:

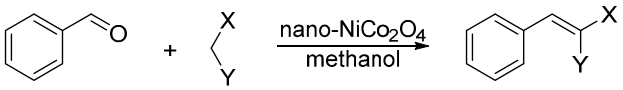

Entry	Benzaldehyde	X	Y	Time (h)	Conversion (%)	Yield (%)		Melting point (°C)	
						$NiCo_2O_4$ [b]	Blank	Experimental	Reported
1	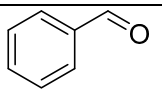	CN	CN	5	99	99	77	84.3–84.5	83–85
2	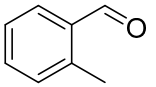	CN	CN	1.5	99	99	27	107.1–107.2	104–106
3	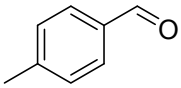	CN	CN	1.5	99	99	74	136.8–136.9	134
4	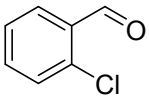	CN	CN	1	99	99	37	95.7–95.8	95–96
5	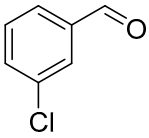	CN	CN	1	99	99	43	117.9–118.1	117–118
6	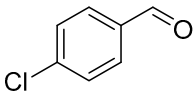	CN	CN	1	99	99	38	163.1–163.3	162–163
7	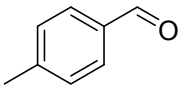	CN	COOEt	9	99	99	5	93.1–93.6	92–93
8	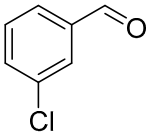	CN	COOEt	12	99	99	14	102.7–102.8	102–103
9	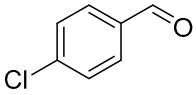	CN	COOEt	11	99	99	5	92.0–92.4	91–93

[a] Reaction conditions: benzaldehyde, 1.0 mmol; malononitrile or ethyl cyanoacetate, 1.2 mmol; $NiCo_2O_4$ catalyst, 8% in mol; solvent (methanol), 2 mL; room temperature. [b] The products were analyzed by GC and ^{1}H NMR

3.5 Possible reaction mechanism

We investigated the possible catalytic mechanism of the Knoevenagel condensation between benzaldehyde and malononitrile with respect to the acidic and basic sites of $NiCo_2O_4$ (Fig. 16). A few published reports have proposed a combined acid-base-catalyzed mechanism for the Knoevenagel condensation based on density functional theory (DFT) calculations and kinetic study (Boronat et al., 2010). The proposed mechanism could comprise two steps: deprotonation of adsorbed malononitrile and co-adsorbption of benzaldehyde to form a condensation

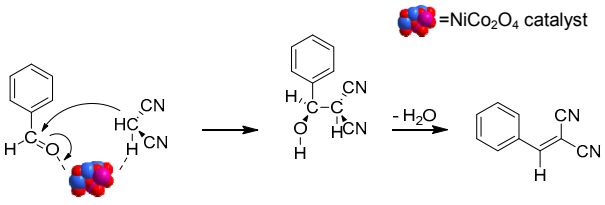

Fig. 16 Possible mechanism for $NiCo_2O_4$ catalyzed Knoevenagel condensation

intermediate. In the presence of the bifunctional $NiCo_2O_4$, a transition state occurs in a lower activation barrier in the C-C bond-forming process. Finally, the intermediate dehydrates to produce the terminal product.

4 Conclusions

In summary, a convenient and environmentally-friendly procedure is provided for the synthesis of 2-benzylidenemalononitrile by Knoevenagel condensation of benzaldehyde and malononitrile using nano-$NiCo_2O_4$ as a new, effective, stable, and recyclable catalyst. In practice, this advanced catalyst can achieve not only superior catalytic performance, but also a favourable number of cycles. Thus, it has considerable potential for application to continuous Knoevenagel condensation reactions without significant loss of catalytic activity.

Contributors

Yang-yang FANG wrote the first draft of the manuscript and performed the tests. Xiao-zhong WANG, Ying-qi CHEN, and Li-yan DAI supervised the research work and revised and edited the final version.

Conflict of interest

Yang-yang FANG, Xiao-zhong WANG, Ying-qi CHEN, and Li-yan DAI declare that they have no conflict of interest.

References

Adisakwattana S, Moonsan P, Yibchok-Anun S, 2008. Insulin-releasing properties of a series of cinnamic acid derivatives in vitro and in vivo. *Journal of Agricultural and Food Chemistry*, 56(17):7838-7844. https://doi.org/10.1021/jf801208t

Ali I, Haque A, Saleem K, et al., 2013. Curcumin-I Knoevenagel's condensates and their Schiff's bases as anticancer agents: synthesis, pharmacological and simulation studies. *Bioorganic & Medicinal Chemistry*, 21(13):3808-3820. https://doi.org/10.1016/j.bmc.2013.04.018

Boronat M, Climent MJ, Corma A, et al., 2010. Bifunctional acid-base ionic liquid organocatalysts with a controlled distance between acid and base sites. *Chemistry*, 16(4): 1221-1231. https://doi.org/10.1002/chem.200901519

Burri DR, Shaikh IR, Choi KM, et al., 2007. Facile heterogenization of homogeneous ferrocene catalyst on SBA-15 and its hydroxylation activity. *Catalysis Communications*, 8(4):731-735. https://doi.org/10.1016/j.catcom.2006.09.006

Chen XW, Li XH, Song HB, et al., 2008. Synthesis of a basic imidazolide ionic liquid and its application in catalyzing Knoevenagel condensation. *Chinese Journal of Catalysis*, 29(10):957-959. https://doi.org/10.1016/S1872-2067(08)60078-9

Dai L, Cao CX, Gao YF, et al., 2011. Synthesis and phase transition behavior of undoped VO_2 with a strong nano-size effect. *Solar Energy Materials and Solar Cells*, 95(2):712-715. https://doi.org/10.1016/j.solmat.2010.10.008

El Baydi M, Tiwari SK, Singh RN, et al., 1995. High specific surface area nickel mixed oxide powders $LaNiO_3$ (perovskite) and $NiCo_2O_4$ (spinel) via sol-gel type routes for oxygen electrocatalysis in alkaline media. *Journal of Solid State Chemistry*, 116(1):157-169. https://doi.org/10.1006/jssc.1995.1197

Gao Z, Zhou J, Cui FM, et al., 2010. Superparamagnetic mesoporous Mg-Fe bi-metal oxides as efficient magnetic solid-base catalysts for Knoevenagel condensations. *Dalton Transactions*, 39(46):11132-11135. https://doi.org/10.1039/c0dt00710b

Gawande MB, Jayaram RV, 2006. A novel catalyst for the Knoevenagel condensation of aldehydes with malononitrile and ethyl cyanoacetate under solvent free conditions. *Catalysis Communications*, 7(12):931-935. https://doi.org/10.1016/j.catcom.2006.03.008

Ghomi JS, Akbarzadeh Z, 2018. Ultrasonic accelerated Knoevenagel condensation by magnetically recoverable $MgFe_2O_4$ nanocatalyst: a rapid and green synthesis of coumarins under solvent-free conditions. *Ultrasonics Sonochemistry*, 40:78-83. https://doi.org/10.1016/j.ultsonch.2017.06.022

Hua YM, Hu WM, 2004. Rapid synthesis of ZSM-5 zeolite catalyst for amination of ethanolamine. *Journal of Zhejiang University-SCIENCE*, 5(6):705-708. https://doi.org/10.1007/BF02840984

Jameel U, Zhu MQ, Chen XZ, et al., 2016. Green epoxidation of cyclooctene with molecular oxygen over an eco-friendly heterogeneous polyoxometalate-gold catalyst $Au/BW_{11}/Al_2O_3$. *Journal of Zhejiang University-SCIENCE A (Applied Physics & Engineering)*, 17(12):1000-1012. https://doi.org/10.1631/jzus.A1500332

Jiang H, Wang M, Song ZG, et al., 2009. Inorganic zinc salts catalyzed Knoevenagel condensation at room temperature without solvent. *Preparative Biochemistry & Biotechnology*, 39(2):194-200. https://doi.org/10.1080/10826060902800866

Kaikhosravi M, Hadadzadeh H, Katani S, 2016. $NiCo_2O_4$ nanospinel and its catalytic activity for oxidation of Rhodamine B at ambient conditions. *Materials Chemistry and Physics*, 170:62-70. https://doi.org/10.1016/j.matchemphys.2015.12.019

Karaoğlu E, Baykal A, Şenel M, et al., 2012. Synthesis and

characterization of piperidine-4-carboxylic acid functionalized Fe_3O_4 nanoparticles as a magnetic catalyst for Knoevenagel reaction. *Materials Research Bulletin*, 47(9):2480-2486. https://doi.org/10.1016/j.materresbull.2012.05.015

Kasralikar HM, Jadhavar SC, Bhusare SR, et al., 2015. Synthesis and molecular docking studies of oxochromenyl xanthenone and indolyl xanthenone derivatives as anti-HIV-1 RT inhibitors. *Bioorganic & Medicinal Chemistry Letters*, 25(18):3882-3886. https://doi.org/10.1016/j.bmcl.2015.07.050

Khan D, Mukhtar S, Alsharif MA, et al., 2017. $PhI(OAc)_2$ mediated an efficient Knoevenagel reaction and their synthetic application for coumarin derivatives. *Tetrahedron Letters*, 58(32):3183-3187. https://doi.org/10.1016/j.tetlet.2017.07.018

Ladipo FT, Anderson GK, 1994. Convenient method for the synthesis of chloro-bridged methyl- and acetylpalladium(II) dimers. *Organometallics*, 13(1):303-306. https://doi.org/10.1021/om00013a044

Li QC, Wang XZ, Yu YY, et al., 2016. Tailoring a magnetically separable $NiFe_2O_4$ nanoparticle catalyst for Knoevenagel condensation. *Tetrahedron*, 72(50):8358-8363. https://doi.org/10.1016/j.tet.2016.11.011

Liu JB, Shi HJ, Shen Q, et al., 2017. A biomimetic photoelectrocatalyst of Co–porphyrin combined with a g-C_3N_4 nanosheet based on π–π supramolecular interaction for high-efficiency CO_2 reduction in water medium. *Green Chemistry*, 19(24):5900-5910. https://doi.org/10.1039/C7GC02657A

Lu T, Chen FW, 2012. Multiwfn: a multifunctional wavefunction analyzer. *Journal of Computational Chemistry*, 33(5):580-592. https://doi.org/10.1002/jcc.22885

Mahmoudi H, Malakooti R, 2014. Solvent free highly dispersed zinc oxide within confined space of Al-containing SBA-15 as an efficient catalyst for Knoevenagel condensation. *Letters in Organic Chemistry*, 11(6):457-464. https://doi.org/10.2174/15701786116666140218004037

Modak A, Mondal J, Bhaumik A, 2013. Porphyrin based porous organic polymer as bi-functional catalyst for selective oxidation and Knoevenagel condensation reactions. *Applied Catalysis A: General*, 459:41-51. https://doi.org/10.1016/j.apcata.2013.03.036

Pang MJ, Jiang S, Long GH, et al., 2016. Mesoporous $NiCo_2O_4$ nanospheres with a high specific surface area as electrode materials for high-performance supercapacitors. *RSC Advances*, 6(72):67839-67848. https://doi.org/10.1039/C6RA14099H

Rubio-Clemente A, Chica E, Peñuela GA, 2015. Petrochemical wastewater treatment by photo-Fenton process. *Water, Air, & Soil Pollution*, 226:62. https://doi.org/10.1007/s11270-015-2321-x

Sharma N, Sharma A, Shard A, et al., 2011. Tandem allylic oxidation-condensation/esterification catalyzed by silica gel: an expeditious approach towards antimalarial diaryldienones and enones from natural methoxylated phenylpropenes. *Organic & Biomolecular Chemistry*, 9(14):5211-5219. https://doi.org/10.1039/C1OB05293D

Sharona H, Loukya B, Bhat U, et al., 2017. Coexisting nanoscale inverse spinel and rock salt crystallographic phases in $NiCo_2O_4$ epitaxial thin films grown by pulsed laser deposition. *Journal of Applied Physics*, 122(22):225301. https://doi.org/10.1063/1.4998776

Sirotin SV, Moskovskaya IF, Romanovsky BV, 2011. Synthetic strategy for Fe-MCM-41 catalyst: a key factor for homogeneous or heterogeneous phenoloxidation. *Catalysis Science & Technology*, 1(6):971-980. https://doi.org/10.1039/c1cy00107h

Sun Q, Shi LX, Ge ZM, et al., 2005. An efficient and green procedure for the Knoevenagel condensation catalyzed by urea. *Chinese Journal of Chemistry*, 23(6):745-748. https://doi.org/10.1002/cjoc.200590745

Taher A, Lee DJ, Lee BK, et al., 2016. Amine-functionalized metal-organic frameworks: an efficient and recyclable heterogeneous catalyst for the Knoevenagel condensation reaction. *Synlett*, 27(9):1433-1437. https://doi.org/10.1055/s-0035-1561356

Tamaddon F, Azadi D, 2017. Preparation of a superior liquid catalyst by hybridization of three solids of nanoZnO, urea, and choline chloride for Knoevenagel-based reactions. *Journal of the Iranian Chemical Society*, 14(10):2077-2086. https://doi.org/10.1007/s13738-017-1144-7

Texier-Boullet F, Foucaud A, 1982. Knoevenagel condensation catalysed by aluminium oxide. *Tetrahedron Letters*, 23(47):4927-4928. https://doi.org/10.1016/S0040-4039(00)85749-4

Tryambake PT, 2017. Microwave assisted urea-acetic acid catalyzed Knoevenagel condensation of ethyl cyanoacetate and 1,3-thiazolidine-2,4-dione with aromatic aldehydes under solvent free condition. *Asian Journal of Chemistry*, 29(11):2401-2405. https://doi.org/10.14233/ajchem.2017.20695

Viveka S, Vasantha G, Dinesha, et al., 2016. Structural, spectral, and theoretical investigations of 5-methyl-1-phenyl-1*H*-pyrazole-4-carboxylic acid. *Research on Chemical Intermediates*, 42(5):4497-4511. https://doi.org/10.1007/s11164-015-2292-y

Voge HH, Good GM, 1949. Thermal cracking of higher paraffins. *Journal of the American Chemical Society*, 71(2):593-597. https://doi.org/10.1021/ja01170a059

Wang SX, Li JT, Yang WZ, et al., 2002. Synthesis of ethyl α-cyanocinnamates catalyzed by KF-Al_2O_3 under ultrasound irradiation. *Ultrasonics Sonochemistry*, 9(3):159-161.

https://doi.org/10.1016/S1350-4177(01)00115-8

Xie J, Chen L, Au CT, et al., 2015. Synthesis of KOH/SnO_2 solid superbases for catalytic Knoevenagel condensation. *Catalysis Communications*, 66:30-33. https://doi.org/10.1016/j.catcom.2015.03.008

Xu J, Shen K, Xue B, et al., 2013. Microporous carbon nitride as an effective solid base catalyst for Knoevenagel condensation reactions. *Journal of Molecular Catalysis A: Chemical*, 372:105-113. https://doi.org/10.1016/j.molcata.2013.02.019

Xue B, Liu XM, Liu N, et al., 2018. A simple strategy to prepare graphene oxide modified by ammonia gas catalysts for Knoevenagel condensation. *Research on Chemical Intermediates*, 44(3):1523-1536. https://doi.org/10.1007/s11164-017-3182-2

Yang PK, Liu YW, Chai L, et al., 2018. Nmp-based ionic liquids: recyclable catalysts for both hetero-Michael addition and Knoevenagel condensation in water. *Synthetic Communications*, 48(9):1060-1067. https://doi.org/10.1080/00397911.2018.1434544

Ying AG, Wang LM, Qiu FL, et al., 2015. Magnetic nanoparticle supported amine: an efficient and environmental benign catalyst for versatile Knoevenagel condensation under ultrasound irradiation. *Comptes Rendus Chimie*, 18(2):223-232. https://doi.org/10.1016/j.crci.2014.05.012

Zhang F, Yang XS, Jiang L, et al., 2013. Piperazine-functionalized ordered mesoporous polymer as highly active and reusable organocatalyst for water-medium organic synthesis. *Green Chemistry*, 15(6):1665-1672. https://doi.org/10.1039/C3GC40215K

Zhang Y, Xia CG, 2009. Magnetic hydroxyapatite-encapsulated γ-Fe_2O_3 nanoparticles functionalized with basic ionic liquids for aqueous Knoevenagel condensation. *Applied Catalysis A: General*, 366(1):141-147. https://doi.org/10.1016/j.apcata.2009.06.041

中文概要

题　目：高效的磁性 $NiCo_2O_4$ 纳米粒子催化脑文格尔缩合反应的研究

目　的：脑文格尔缩合反应已被广泛应用于精细化学品、药物、香料和化妆品等领域，是重要的有机合成反应之一。传统的缩合反应存在催化剂稳定性差、分离难、催化活性低等问题。本文旨在探讨 $NiCo_2O_4$ 的制备方法与结构的关系和催化剂用于脑文格尔缩合反应的条件对性能的影响。

创新点：1. 通过采用不同的煅烧温度，确定合成 $NiCo_2O_4$ 尖晶石催化剂的最适温度，以减少 NiO 的生成；2. 优化反应条件，使苯甲醛和丙二腈的缩合反应收率达到 99%；3. 获得的 $NiCo_2O_4$ 催化剂的稳定性很高，在循环 20 次后催化性能仍保持不变。

方　法：1. 通过 X 射线单晶衍射和傅里叶红外光谱分析，推断在不同煅烧温度下合成的催化剂的组成，并确定最佳煅烧温度（图 2 和 3）；2. 对 $NiCo_2O_4$ 尖晶石催化剂进行透射电镜、二氧化碳/氨气程序升温脱附和氮气吸脱附表征，探究其微观结构与性能之间的关系（图 4~8）；3. 通过苯甲醛和丙二腈的脑文格尔缩合反应，验证催化剂的活性。

结　论：1. 成功合成出高效的磁性 $NiCo_2O_4$ 纳米颗粒；2. 以脑文格尔缩合反应作为探针反应，发现 $NiCo_2O_4$ 具有高催化性能，并且其反应转化率和收率高达 99%；3. 催化剂具有磁性，易于回收；4. 在循环 20 次后，反应活性不变，说明催化剂具有高稳定性。

关键词：$NiCo_2O_4$ 催化剂；尖晶石；脑文格尔缩合反应；非均相催化